

## ALKALI FELDSPAR IN THE PERALUMINOUS SOUTH MOUNTAIN BATHOLITH, NOVA SCOTIA: TRACE-ELEMENT DATA

DANIEL J. KONTAK<sup>1</sup>

*Nova Scotia Department of Natural Resources, P.O. Box 698, Halifax, Nova Scotia B3J 2T9*

ROBERT F. MARTIN<sup>1</sup>

*Department of Earth and Planetary Sciences, McGill University, 3450 University Street, Montreal, Quebec H3A 2A7*

### ABSTRACT

Alkali feldspar separates ( $n = 52$ ) from the eastern part of the Late Devonian, peraluminous South Mountain Batholith of Nova Scotia, in eastern Canada, have been analyzed from the relatively primitive, early granodiorite, through monzogranite, to evolved pegmatites hosted by leucogranites. The alkali feldspar, with bulk compositions ( $Or_{55-80}$ ) consistent with magmatic conditions, shows systematic variations in trace-element content; levels of Ba, Sr, Pb, the rare earths, Th, and Zr decrease, and concentrations of Rb, Cs, and Ga increase, in alkali feldspar in the sequence granodiorite – monzogranite – pegmatite. The continuity and trajectory of trends in binary and element-ratio diagrams follow the trend predicted for Rayleigh fractional crystallization, as do linear trends in log-log plots. In chondrite-normalized plots, the rare-earth elements decrease continuously, along with  $Eu_N/Eu^*$ , reflecting the fractionation of accessory minerals. Modeling of the trace-element populations give  $F$  values consistent with the observed proportions of rock types in the batholith. The chondrite-normalized profiles of alkali feldspar from evolved rocks indicate an inflexion in the concentration of the heavy rare-earths and anomalies involving the most mobile trace elements. It seems clear that these elements were complexed by a fluid phase, which likely also was involved in localized lithophile-element mineralization and related metasomatism.

**Keywords:** alkali feldspar, geochemistry, pegmatites, granites, South Mountain Batholith, Nova Scotia.

### SOMMAIRE

Nous avons analysé des concentrés de feldspath alcalin ( $n = 52$ ) d'une suite de roches allant de granodiorite précoce, en passant par monzogranite, jusqu'à pegmatites évoluées mises en place dans les monzogranites, provenant de la partie orientale du batholite de South Mountain, en Nouvelle-Écosse. Le feldspath alcalin a une composition globale ( $Or_{55-80}$ ) conforme à une cristallisation magmatique; il montre des variations systématiques en teneurs en éléments traces. Par exemple, les teneurs en Ba, Sr, Pb, terres rares, Th et Zr diminuent, et les teneurs en Rb, Cs et Ga augmentent dans le feldspath alcalin de la séquence granodiorite – monzogranite – pegmatite. La continuité et l'allure des tracés dans des diagrammes binaires et en termes de rapports d'éléments, ou bien encore dans des diagrammes log-log, sont largement conformes au modèle de cristallisation fractionnée selon Rayleigh. Les concentrations des terres rares, normalisées par rapport à une chondrite, diminuent progressivement, de même que  $Eu_N/Eu^*$ , résultat du fractionnement progressif de minéraux accessoires. Le modèle prédit des valeurs de  $F$  conformes à la proportion de roches observée dans le batholite. En revanche, dans certains cas, le feldspath alcalin des roches les plus évoluées montre une inflexion dans les concentrations de terres rares lourdes, ainsi que des écarts impliquant les éléments les plus mobiles. Il semble donc que ces éléments aient été transportés par l'intermédiaire d'une phase fluide, qui a aussi localement mené à une minéralisation en éléments lithophiles et une métasomatose associée.

**Mots-clés:** feldspath alcalin, géochimie, pegmatites, granites, batholite de South Mountain, Nouvelle-Écosse.

### INTRODUCTION

The South Mountain Batholith (SMB), southern Nova Scotia (Fig. 1), is a large (7,300 km<sup>2</sup>), peraluminous Devonian-Carboniferous intrusion containing an early granodiorite phase and progressively more evolved rocks, leading to leucogranite and associated pegmatites

(Clarke & Muecke 1985, Clarke & Chatterjee 1988, MacDonald *et al.* 1992). Lithophile-element and base-metal mineralization and deuteric alteration are associated with the more evolved units (*e.g.*, Kontak & Corey 1988, MacDonald *et al.* 1992). The SMB is now considered one of the best characterized examples of peraluminous felsic magmatism. Recently, Kontak *et al.* (1996) presented the

<sup>1</sup> E-mail addresses: djkontak@gov.ns.ca, bob\_m@geosci.lan.mcgill.ca

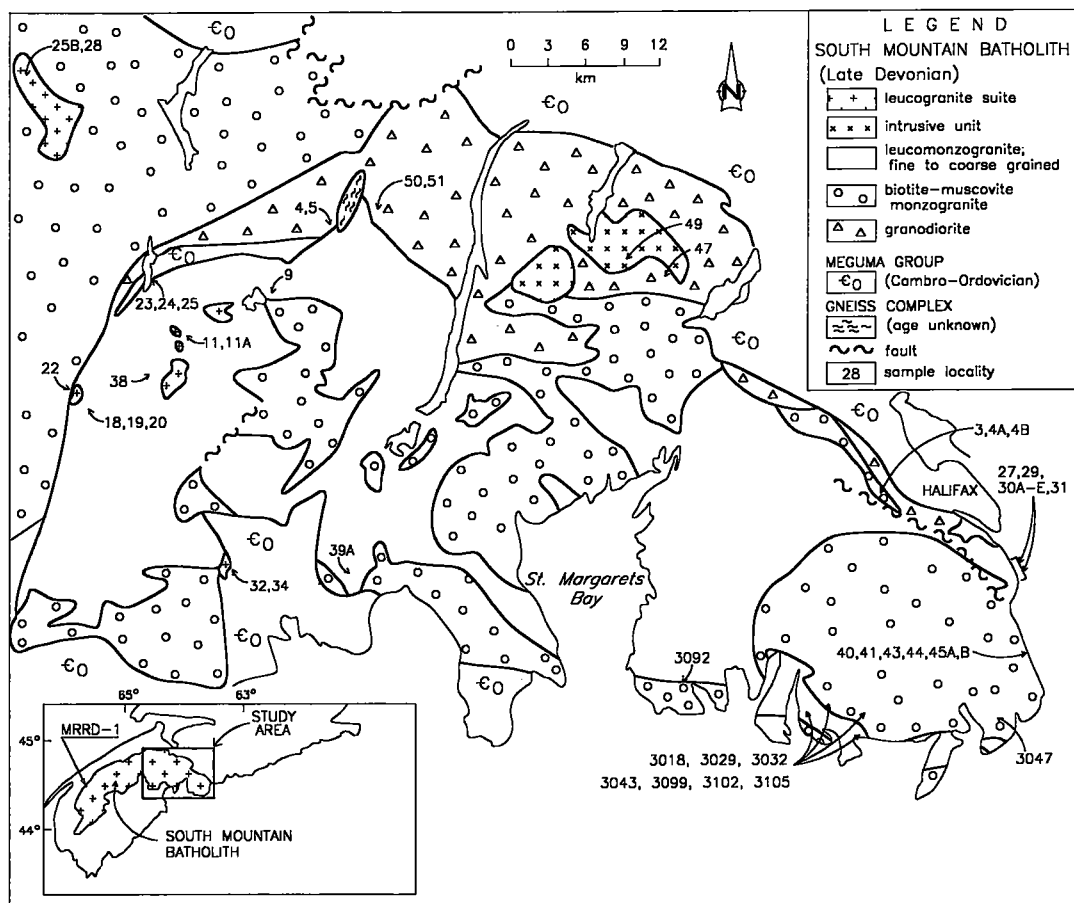


FIG. 1. Geological map for the eastern part of the South Mountain Batholith, with sample locations indicated. Geology is simplified after MacDonald *et al.* (1992). Fresh granodiorite also was sampled in drill hole MRRD-1 (Clarke & Chatterjee 1988).

results of a crystal-chemical study of alkali feldspar in the eastern part of the SMB, with the focus on degree of Al-Si order and P content of bulk separates and of K- and Na-rich exsolution-related domains. Here, the focus is on trace-element geochemistry of the same suite of feldspar separates. As in the previous contribution, our purpose is to decipher the respective roles of feldspar-melt and feldspar-fluid equilibria. The results are discussed in the context of geochemical and stable isotopic data (Kontak *et al.* 1988, 1991) on a similar suite of whole-rock samples and mineral separates.

#### GEOLOGICAL SETTING OF THE SOUTH MOUNTAIN BATHOLITH

The SMB intrudes Lower Paleozoic metasedimentary rocks of the Meguma Group, a thick turbiditic sequence dominated by sandstone and shale. The Meguma Group rocks and overlying Silurian-Devonian volcano-sedimentary rocks were regionally deformed and

metamorphosed (greenschist to amphibolite facies) during the Devonian (*ca.* 400 Ma) Acadian Orogeny. Emplacement of the batholith occurred at *ca.* 370 Ma (Reynolds *et al.* 1987, Clarke *et al.* 1993), at a depth equivalent to 3 kbars pressure, based on the presence of magmatic muscovite and andalusite (Clarke *et al.* 1976) and contact-metamorphic assemblages (Raeside & Mahoney 1996). The concordance of U/Pb, Rb/Sr and  $^{40}\text{Ar}/^{39}\text{Ar}$  radiometric ages (MacDonald *et al.* 1992) suggests rapid post-emplacement cooling, in agreement with the dominance of stranded orthoclase in the batholith (Kontak *et al.* 1996). The batholith was unroofed by the Famennian-Tournaisian, as terrestrial clastic material of the Horton Group rests on the granite.

MacDonald *et al.* (1992) subdivided the SMB into granodiorite, monzogranite, leucomonzogranite and leucogranite, and recognized several separate intrusive centers. Field relationships indicate that a granodiorite-monzogranite envelope was emplaced first. The distribution of rocks types and trend-surface analysis of

## ANALYTICAL TECHNIQUES

compositional data indicate that each intrusive center evolved independently (*e.g.*, MacDonald & Horne 1988). Bodies of pegmatite may occur in all units of the SMB, but are more abundant in the evolved units.

In the Halifax intrusive center, two varieties of monzogranite have been distinguished in the field (MacDonald & Horne 1988), and are discussed separately here. The Harrietsfield biotite monzogranite, characterized by the presence of trace amounts of muscovite and cordierite, intrudes the Halifax leucomonzogranite. The contact between these two variants in places seems gradational, which implies that these two batches of magma probably were coeval, and mixed along part of their common boundary.

## LOCALITIES SAMPLED AND PETROGRAPHY

Samples of alkali feldspar (AF) were collected from all phases of the eastern SMB (Fig. 1) except the leucogranites, which are too fine grained to give

High-quality separates ( $n = 52$ , Table 1; note that NS-86-4A and NS-86-4B represent duplicate sampling of two different localities) of AF were prepared by pulverizing and sieving ( $-20$  to  $+65$  mesh), followed by hand picking under a binocular microscope and cleaning with deionized water. The separates, which are free of inclusions (*e.g.*, biotite), were prepared for chemical analysis by crushing to  $-200$  mesh. Concentrations of the trace elements, including the rare-earth elements (*REE*), were determined by inductively coupled plasma – mass spectrometry (ICP-MS) at the Memorial University of Newfoundland using procedures outlined in Jenner *et al.* (1990). To assess the potential variation due to heterogeneity, two separates were each analyzed eight or nine times. The results of these replications, reported elsewhere (Kontak 1995), indicate that neither size nor heterogeneity of samples was an inherent problem in the chemical analysis of the separates.

## TRACE-ELEMENT GEOCHEMISTRY OF THE ALKALI FELDSPAR

The separates of alkali feldspar from the sequence granodiorite to evolved pegmatite define a bulk composition in the range  $Or_{60}$  to  $Or_{80}$  (Fig. 2), with a tendency for the AF in granodiorite to be more potassic than the AF in monzogranite. This finding may seem counterintuitive, but conforms to phase relationships in the system  $An-Ab-Or-Qtz-H_2O$  (*e.g.*, Černý 1994, Černý *et al.* 1984). The coexisting plagioclase, not characterized in this study, becomes progressively more sodic. The trend of K depletion then is reversed, as the AF in pegmatitic samples emplaced in leucogranitic host-rocks is systematically more potassic than the AF in monzogranite samples.

Trace-element data for the AF separates (Table 1) are summarized in Figure 3, where the data are presented in six groupings, as described above. Except for the *REE*, which merit a separate discussion, results are presented in the sequence monovalent cation to tetravalent cation, and are immediately followed by a crystal-chemical interpretation.

*Rubidium*

Rubidium, the trace element most similar to K, shows a large overall range, from *ca.* 200 ppm to about 2000 ppm, with a progressive enrichment from granodiorite to type-II pegmatites. Note that (1) AF from the Halifax monzogranite is slightly enriched compared to that in the Harrietsfield monzogranite, in keeping with the Ba and Sr trends noted below, (2) the overall trend of Rb enrichment is closer to being exponential than linear, and (3) the enrichment of Rb is not as marked as the depletion noted for Ba and Sr. The concentrations of Rb in AF from the pegmatites in this suite are similar to

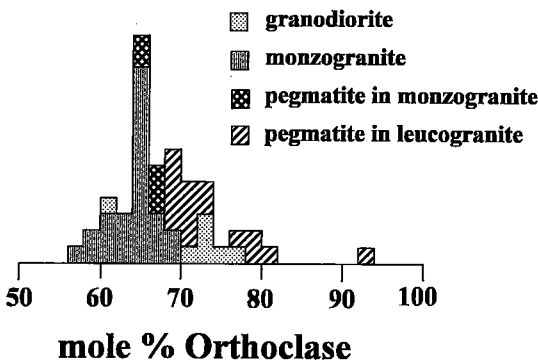


FIG. 2. Histogram (stacked type) summarizing the bulk compositions of alkali feldspar separates (in mole % Or) from the eastern South Mountain Batholith. Square represents result of one analysis.

high-purity separates. In addition, a sample of extremely fresh granodiorite was taken from a drill hole (MRRD-1) in the southwestern part of the batholith (Fig. 1). Details of the sampling are given in Kontak *et al.* (1988, 1991, 1996). Data on the samples of AF are separated, for plotting purposes, into six groups: granodiorite, monzogranite of the Harrietsfield map-unit, monzogranite from the Halifax map-unit, both of the Halifax intrusive center, pegmatite hosted by either monzogranite, and two groupings (I, II) of pegmatite hosted by leucogranitic rocks, group-II pegmatites being the more evolved. The separates all consist of fresh perthitic alkali feldspar, in many cases "glassy". In samples of granodiorite and monzogranite, the AF is coarse (to 2–4 cm), and subhedral to euhedral. Inclusions of biotite may be randomly or concentrically oriented.

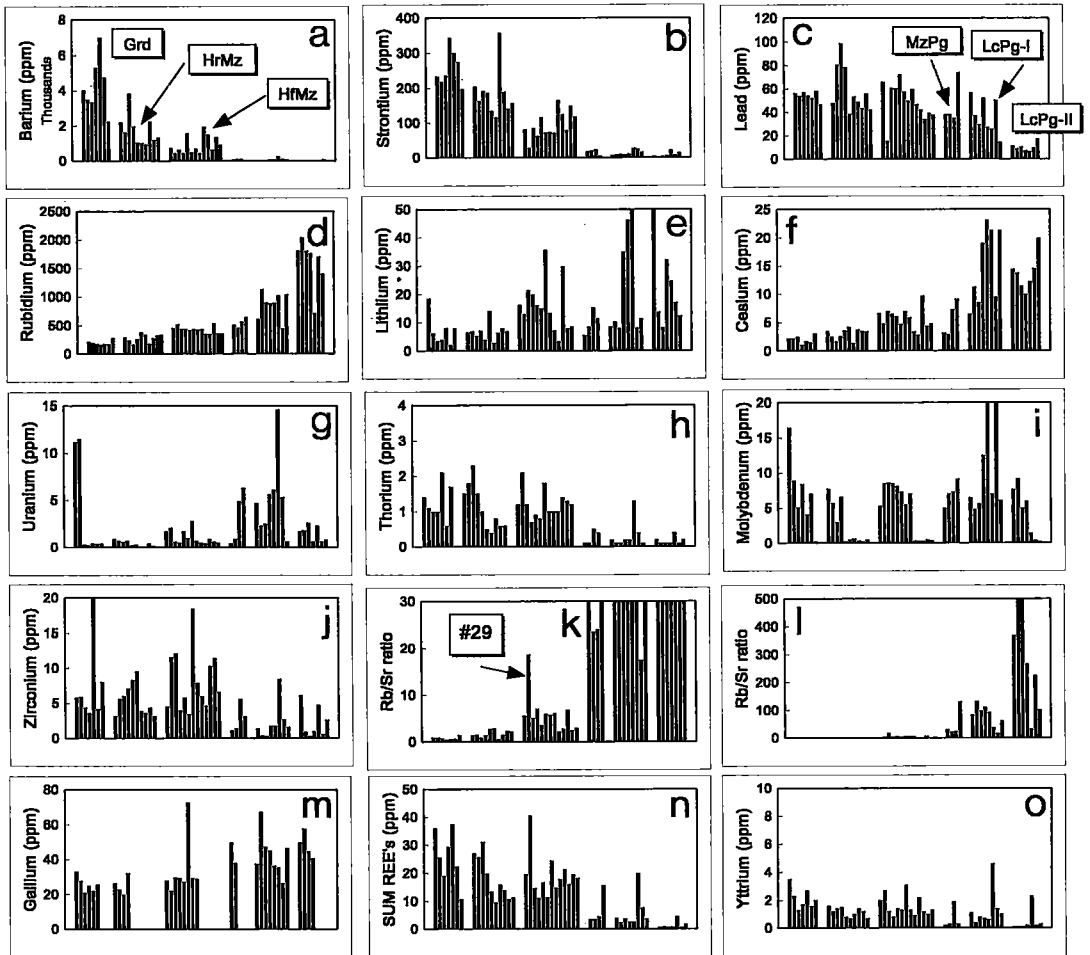


FIG. 3. Histograms summarizing the trace-element geochemistry of alkali feldspar separates ( $n = 52$ ) from various units of the eastern South Mountain Batholith. From left to right on the diagrams, the units are: Granodiorite (Grd), Harrietsfield Monzogranite (HrMz), Halifax Monzogranite (HfMz), Monzogranitic Pegmatites (MzPg), Leucogranitic Pegmatite of type I (LcPgI) and of type II (LcPgII). The significance of sample 29 from the Halifax monzogranite is discussed in the text.

those noted for the onset of pegmatite formation in other batholithic suites (*e.g.*, Harney Peak granite: Shearer *et al.* 1987), and fall far short of the concentrations recorded in highly fractionated rare-element granitic pegmatite systems (*e.g.*, close to 3%  $Rb_2O$  in perthite in the Volta Grande granitic pegmatite, Minas Gerais, Brazil: Lagache & Quéménéur 1997).

#### Cesium

There is a systematic increase in Cs from 2–3 ppm in AF from granodiorite, to 3–7 ppm in AF from monzogranitic and related pegmatitic samples, to 10–22 ppm in AF from the evolved pegmatitic samples, although the buildup is more erratic than for Rb. As in the case of Rb, such concentrations are typical of AF in

the least evolved granitic pegmatites (Černý 1994). In the Volta Grande granitic pegmatite, in spite of very high concentrations of Cs in AF, in the range 500–1400 ppm, Lagache & Quéménéur (1997) again noted the inherent variability in levels of Cs attained. In view of its large ionic radius, and as a consequence, its very large partition-coefficient (40) in favor of a fluid phase (Carron & Lagache 1980), the Cs content of the AF is likely to be very easily affected if open-system feldspar–fluid interaction is suspected.

#### Lithium

The abundance of Li in AF is generally erratic, but there is overall enrichment from *ca.* 5–10 ppm to *ca.* 20 ppm, with progressive evolution to pegmatites.

There is a slight enrichment in AF from the Halifax monzogranite samples compared to AF from the Harrietsfield monzogranite and granodiorite samples. The anomalous enrichment of Li in AF in some pegmatites (to 120 ppm) suggests contamination by micro-inclusions of a Li-bearing phase such as mica. Because of the small ionic radius of Li, the amount of structurally bound Li in AF is very limited, even in more evolved systems; for example, the Rb- and Cs-rich AF in the Volta Grande granitic pegmatite, cited above, which coexists with Li-bearing muscovite, contains a mere 134–154 ppm Li (Lagache & Quéméneur 1997), with the same possibility of micro-inclusions. The highest amounts recorded in Figure 3 thus may well exceed saturation amounts.

#### Barium

Barium is most enriched in AF from granodiorite, although with some scatter (3330 to 7000 ppm). Beyond the granodiorite stage, there is a marked decrease from AF in monzogranite to AF in pegmatite. Among the monzogranite samples, the AF in those from the Harrietsfield map-unit is enriched on average relative to AF from the Halifax map-unit. The strong positive correlation of Ba with mole % Or of the AF (*cf.* Fig. 2) is in keeping with the experimental findings of Icenhower & London (1996).

#### Strontium

The distribution of Sr in AF is generally similar to that of Ba, with maximum enrichment in samples from granodiorite, and relative enrichment in AF from the Harrietsfield monzogranite over AF from the Halifax monzogranite. All samples from pegmatites, including those hosted by monzogranite, show a marked depletion in Sr. The observed trend is consistent with the findings of Icenhower & London (1996).

#### The ratio Rb/Sr

The ratio of Rb and Sr concentrations in AF magnifies the trends for Rb and Sr, with a steady increase over the range granodiorite–monzogranite, and a dramatic increase in the most evolved samples of pegmatite. Note that AF in the Halifax monzogranite has a much higher Rb/Sr value than AF in the Harrietsfield monzogranite. The marked increase in Rb/Sr for AF in pegmatites hosted by monzogranite reflects the very low Sr content.

#### Lead

Samples of AF from granodiorite and monzogranite have similar concentrations at 40 to 60 ppm, whereas AF in pegmatitic samples show generally lower levels and more erratic values, with a marked depletion in the most

evolved (type-II) pegmatites (*i.e.*, <20 ppm). Pb ions are known to be accommodated in K-feldspar in two ways, in a coupled substitution with Al, like Ba and Sr, and also associated with a vacancy, in the place of two K atoms (*e.g.*, Stevenson & Martin 1986). Perhaps because of the role of a second mechanism, the AF in the pegmatitic samples does not show the marked depletion seen with Ba and Sr.

#### Gallium

Although the data-set is incomplete, there is a slight but systematic increase from 20–30 ppm in AF from the less evolved rocks to 40–50 ppm in AF from the more evolved samples. This pattern is in keeping with the general behavior of Ga in granitic suites (Goad & Černý 1981, Černý *et al.* 1985). This element follows Al in the T site in the feldspar structure, and may increase slightly in concentration with increasing evolution, in parallel with the increasing activity of Al in the melt in this batholith.

#### Zirconium

AF separates from granodiorite and monzogranite contain 5–10 ppm, although there are some “spikes”, whereas concentrations in the range <1–2 ppm are more typical of AF in pegmatitic samples, some of these showing lower “spikes”. The trend thus mimics that in whole-rock samples (MacDonald *et al.* 1992). The “spikes” most likely are due to micro-inclusions of zircon. Note that Leeman & Phelps (1981) reported 70–145 ppm Zr in sanidine phenocrysts in rhyolite from the Yellowstone volcanic field, but the inferred partition-coefficient for sanidine–glass, 0.38, seems much too high. Zr may be structurally bound (Smith 1974), but probably at the much lower levels documented here.

#### Molybdenum

There is considerable overall variation in Mo content of the AF, but in general, from <1 to about 10 ppm seem typical. One “spike” is found in AF from the Long Lake molybdenite deposit (177 ppm). Another, in AF from the Walker molybdenite-bearing pegmatite, contains 91 ppm. Both samples were taken from banded pegmatite that contains visible molybdenite mineralization; thus micro-inclusions of molybdenite are considered responsible for the anomalous values.

#### Thorium

The concentration of thorium is uniform at *ca.* 1–2 ppm in AF from granodiorite and monzogranite samples, but there is a striking depletion in AF from the pegmatitic samples.

TABLE 1. CONCENTRATIONS OF TRACE ELEMENTS IN ALKALI FELDSPAR,  
SOUTH MOUNTAIN BATHOLITH, NOVA SCOTIA

Sample	Li	Rb	Sr	Ba	Pb	U	Th	Cs	Mo	Zr	Y	Ga	La	Ce	Pr	Nd	Sm	Eu	Gd	Tb	Dy	Ho	Er	Yb	Lu	
<b>Granodiorite</b>																										
NS-85-4	17	207	228	3940	55	11	1.5	2	16	6	3.3	28	8.1	16.2	1	5.2	1.26	3.2	1.1	0.12	0.65	0.1	0.23	0.39	0.04	
NS-85-5	6.3	194	218	3497	54	12	1.1	2.2	8.9	5.9	2.3	28	6.17	11.7	1.1	3.53	0.92	1.3	0.83	0.08	0.5	0.09	0.19	0.48	0.04	
NS-85-47	3.5	178	236	3330	57	0.3	1	2.5	5.1	4.4	1.3	21	4.1	7.39	0.74	2.49	0.57	2.57	0.45	0.03	0.22	0.04	0.17	0.31	0.03	
NS-85-50	4.1	163	343	5308	54	0.2	1	1.1	8.4	3.6	1.7	25	6.49	11.9	1.06	3.43	0.75	4.07	0.63	0.07	0.28	0.05	0.14	0.43	0.03	
NS-85-51	8.1	175	301	6994	52	0.4	2.1	1.7	4.1	3.1	2.7	22	7.75	15.7	1.49	5.32	1.12	3.76	1.02	0.07	0.47	0.09	0.26	0.55	0.05	
MRRD-1	2.1	173	275	4761	58	0.4	0.6	1.5	7	4.2	1.6	26	4.74	8.05	0.72	2.43	0.65	3.92	0.62	0.04	0.27	0.04	0.14	0.6	0.07	
A16-3043	7.9	284	197	2243	46.5	0.4	1.7	3.1	0.2	8	2	ND	2.57	4.09	0.43	1.5	0.38	0.83	0.38	0.05	0.25	0.05	0.12	0.1	0.12	
<b>Halifax Monzogranite</b>																										
NS-85-27	16.2	451	80.8	725	65.8	1.7	1.2	6.6	5.3	4.6	2	28	4.67	9.24	0.85	2.69	0.7	0.38	0.37	0.04	0.3	0.04	0.16	0.18	0.02	
NS-85-29B	13	523	28.1	432	15.3	2.1	2.1	4.8	8.5	12	2.7	22	9.13	19	1.87	6.37	1.57	0.39	1.04	0.1	0.63	0.07	0.16	0.21	0.03	
NS-85-30A	21.4	436	85.3	652	60.5	0.6	1.2	7	8.6	12	1.2	30	3.62	6.67	0.62	1.98	0.51	0.33	0.29	0.03	0.18	0.04	0.09	0.24	0.02	
NS-85-30B	19.8	445	63	444	60.3	0.5	0.7	6.5	8.5	4	0.8	29	2.87	5.11	0.46	1.38	0.31	0.52	0.2	0.02	0.11	0.02	0.04	0.05	0.02	
NS-85-30C	16.1	418	116	1574	72.2	1.7	0.9	6.1	8.1	5.8	1.4	27	4.31	7.3	0.62	1.86	0.4	1.4	0.29	0.03	0.19	0.02	0.04	0.26	0.02	
NS-85-30D	15	431	72.6	483	57.5	1	0.8	4.7	7.3	3.4	1.3	73	2.85	5.27	0.47	1.52	0.45	1.2	0.39	0.04	0.25	0.03	0.09	0.14	0.01	
NS-85-30E	35.7	426	73.4	694	49.8	2.8	1.8	7	5.5	19	3.1	30	5.46	11.1	1.04	3.56	0.9	0.69	0.57	0.06	0.44	0.07	0.23	0.31	0.04	
NS-85-31	13.3	434	71.6	436	59.6	0.7	1	5.9	7	7.9	1.3	29	3.7	6.7	0.64	2.09	0.53	0.54	0.31	0.03	0.2	0.03	0.1	0.13	0.01	
NS-86-4A2	6.5	356	164	1918	45.3	0.6	1.1	3.4	0.3	4.1	0.9	ND	4.43	7.33	0.81	2.66	0.63	0.92	0.58	0.06	0.31	0.04	0.07	0.03	0.02	
NS-86-4A1	7.9	351	164	1987	47.6	0.4	0.9	3.5	0.2	7	1	ND	4.24	6.83	0.72	2.53	0.58	0.99	0.64	0.06	0.26	0.06	0.09	0.06	0.01	
NS-86-4B	3.4	348	125	1480	42.1	0.4	1	2.8	0.2	4.7	2.2	ND	4.16	8.42	1.08	4.07	1.02	0.67	0.86	0.11	0.53	0.07	0.19	0.14	0.01	
NS-86-4B	2.7	356	122	1516	42.5	0.4	1	2.9	0.3	4.9	2.2	ND	4.24	8.5	1.07	4.11	1	0.73	0.01	0.11	0.56	0.08	0.2	0.13	0.02	
A16-3029	29.7	537	79.1	636	34	0.9	1.4	9.7	0.2	10	1.2	ND	3.53	6.84	0.76	2.77	0.76	0.41	0.55	0.07	0.3	0.04	0.08	0.07	0.01	
A16-3102	7.9	364	148	1355	39.5	0.6	1.3	4.5	0.5	11	1	ND	4.9	8.4	0.85	3.05	0.58	0.81	0.63	0.05	0.28	0.05	0.09	0.06	0.01	
A16-3099	8.5	352	119	924	37.6	0.5	1.2	4.8	0.3	6.6	1.3	ND	4.13	7.4	0.85	3.11	0.73	0.72	0.67	0.08	0.35	0.05	0.13	0.08	0.01	



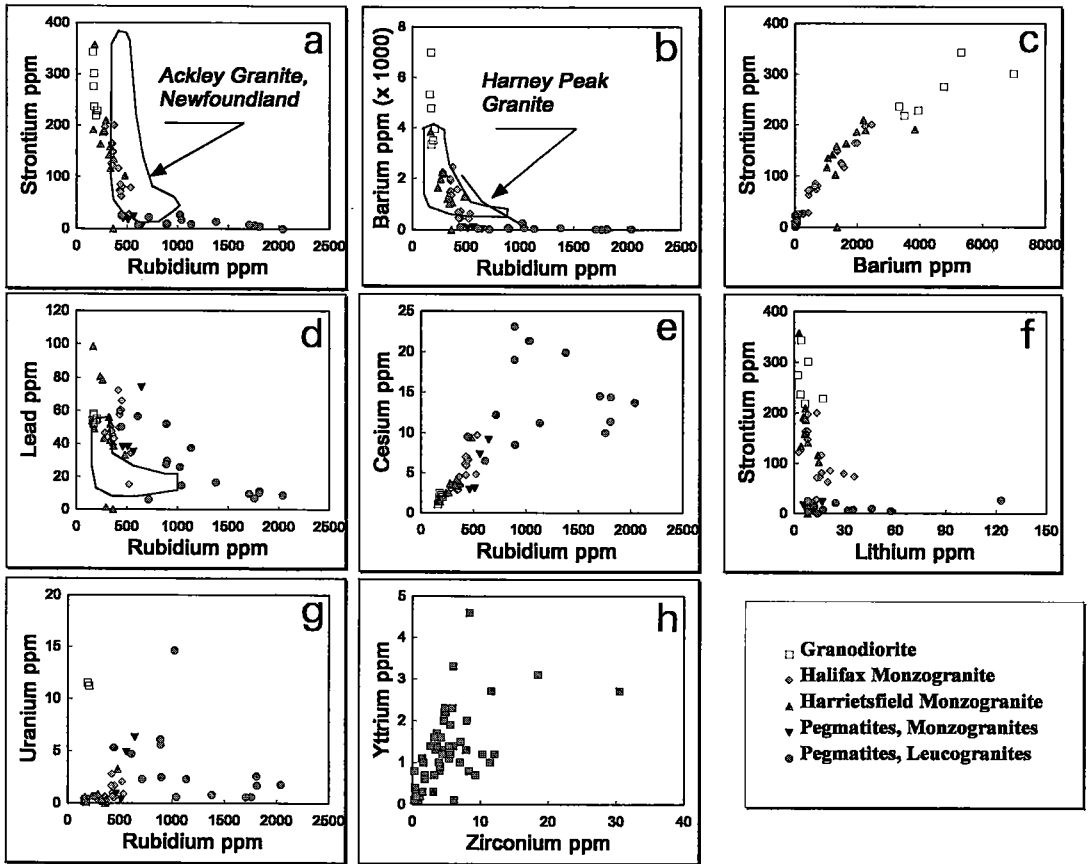


FIG. 4. Binary element plots summarizing trace-element data for alkali feldspar separates from the eastern South Mountain Batholith. The trends for the Ackley Granite and Harney Peak Granite are based on data in Kontak (1995) and Shearer *et al.* (1992), respectively.

### Uranium

The distribution of U is highly variable. Elevated abundances (10 ppm) characterize the AF in two samples of granodiorite, collected near the Millet Brook U deposit (Chatterjee *et al.* 1982), and probably reflects proximity to this mineralization. The enrichment of U in AF from late-stage pegmatites is consistent with the mobility of U associated with the late-stage, evolved phases of the SMB (*e.g.*, Chatterjee *et al.* 1982, Logothetis 1985); we do not consider it structurally bound.

### Binary plots

In Figure 4, the samples generally demonstrate continuous geochemical trends. In plots of Sr and Ba *versus* Rb, there are initially steep trajectories, defined

by granodiorite–monzogranite samples, with a striking leveling off of the trends due to the increase in Rb at constant but low values of both Ba and Sr. There is a clear overlap in the fields for granodiorite- and monzogranite-hosted AF. In the Sr *versus* Rb plot, the trend is nearly identical to the general case for granites and pegmatites (Černý *et al.* 1985). As expected, there is a strong correlation of the data in a Sr *versus* Ba plot, although a break in slope separates the granodiorite samples from the rest. In the Pb *versus* Rb plot, the AF in some of the monzogranite samples is relatively less evolved than AF in granodiorite samples, which are tightly clustered. In the Cs *versus* Rb plot, a well-defined trend is indicated by AF in the granodiorite–monzogranite range. AF from the most evolved (type-II) pegmatites define a trend of increasing Rb at more or less constant Cs, whereas AF in type-I pegmatite is the most enriched in Cs, and lies

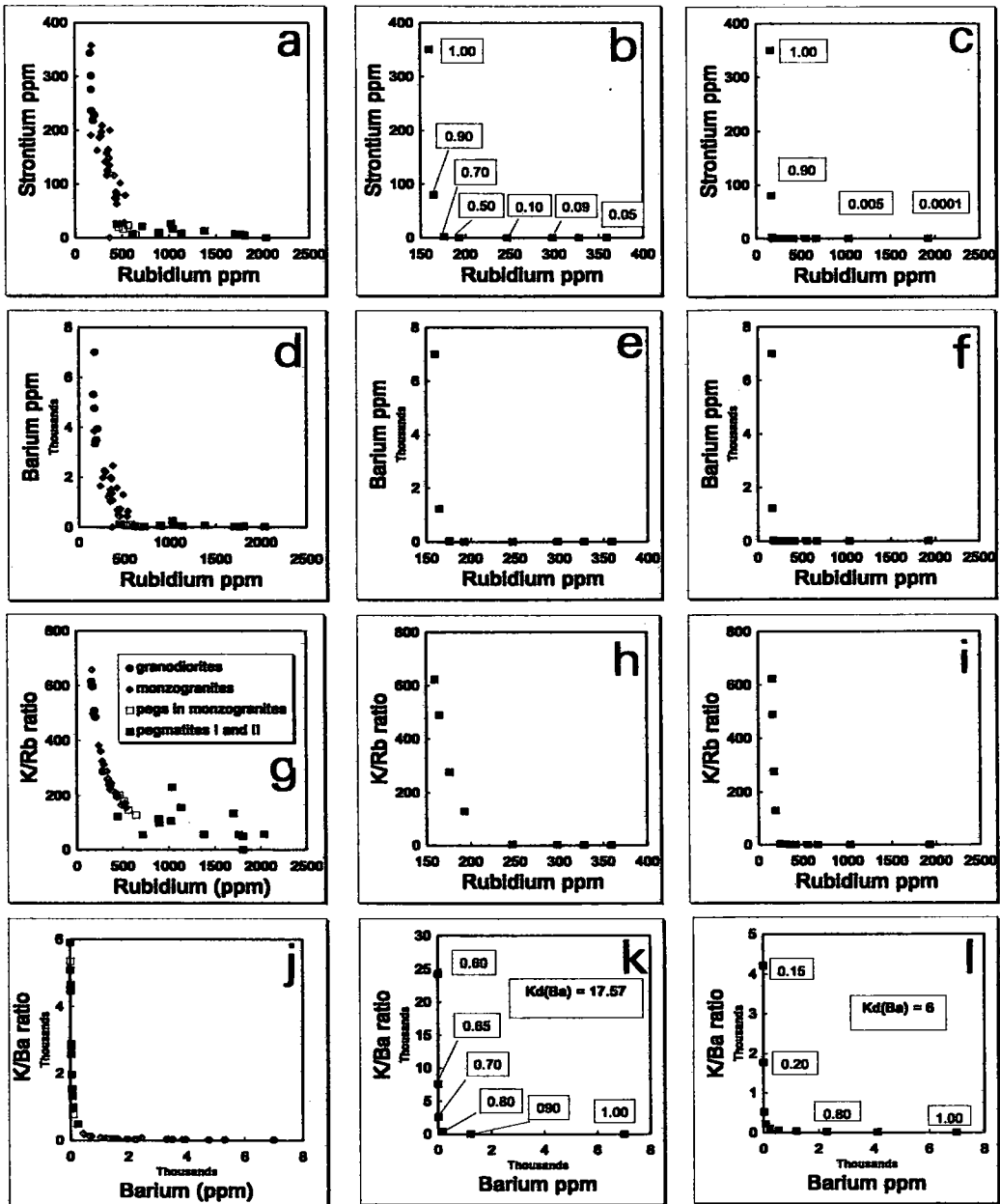


FIG. 5. Binary element and ratio plots for selected trace elements for alkali feldspar separates from the South Mountain batholith; note that there are four subdivisions of the data, as shown inset in the K/Rb versus Rb plot. The plots in the middle and the right are calculated trends assuming Rayleigh crystal fractionation [equations in Hanson (1978)]. The numbers within the boxes in the Sr versus Rb plot are  $F$  values (i.e., weight fraction of melt remaining) and apply to the top three plots (i.e., Sr versus Rb, Ba versus Rb, K/Rb versus Rb), whereas other values are indicated in the K/Ba versus Ba plot. Diagrams on the right illustrate that very low  $F$  values (0.005 to 0.0001) are required to explain the Rb contents of the alkali feldspars. Partition coefficients used are from Icenhower & London (1976) for Rb, Ba and Sr for an average bulk composition of the alkali feldspar of Or70 and a  $K_D$  of 3 for K, as calculated using the bulk composition from this study and Kontak *et al.* (1996), and the whole-rock data for the batholith (MacDonald *et al.* 1992). Note that for the K/Ba versus Ba plot, two partition coefficients have been used (17.57 and 6), as discussed in the text. In Figure 5e, the values of  $F$  are the same as in Figure 5b; in Figure 5f, they are the same as in Figure 5c.

on a continuation of the main trend. These trends for AF from pegmatites conform to those identified for pegmatites associated with leucogranites by Černý *et al.* (1985). In the Sr versus Li plot, there is marked enrichment in Li at very low Sr values. However, the U versus Rb plot indicates that the two elements are decoupled.

As with the other binary plots, the K/Rb versus Rb plot (Fig. 5) shows a continuum from granodiorite to pegmatite. The most evolved samples of AF have a K/Rb value in the range 50–60, typical of leucogranite and relatively unevolved pegmatitic granite (Černý *et al.* 1985, Černý 1992, Shearer *et al.* 1987). In a K/Ba versus Ba plot, there is uniformly low K/Ba within granodiorite–monzogranite samples, again with an overlap of the two data sets, followed by a marked increase in K/Ba for AF from the more evolved rocks.

### The rare-earth elements

Rare-earth-element data for the suite are summarized in Figures 3 and 6. In general, the chondrite-normalized plots resemble patterns for AF from intrusive (*e.g.*, Shearer *et al.* 1987, Smith & Brown 1988, Kontak 1995) and extrusive (Leeman & Phelps 1981) felsic rocks, but there are systematic differences from one rock type to the other. There is a trend of decreasing  $\Sigma REE$  in AF from granodiorite to the evolved pegmatites, with a marked depletion in AF at the pegmatitic stage, for both pegmatites hosted by monzogranites and those hosted by leucogranites (Fig. 3). However, a similar plot for Y shows a more systematic trend of decreasing Y in AF from granodiorite to pegmatite, which reflects the fact that most of the decrease in the REE is due to the light rare-earths (LREE) and not the heavy rare-earths (HREE). In Figure 3, the  $\Sigma REE$  of AF in most monzogranitic samples is comparable to that from granodioritic samples, as in the case of Sr, Th and Pb.

Chondrite-normalized REE plots for the AF from granodiorite and monzogranite are similar (Fig. 6). Both groups show strongly fractionated patterns, LREE enrichment and a positive Eu anomaly. However, the AF samples from the Halifax monzogranite do not have as elevated a  $Eu_N/Eu^*$  value; many of the AF samples from granodiorite and monzogranite have an inflection at Yb and Lu that remains unexplained. Analytical error is an unlikely explanation, as (1) other samples of AF processed with these AF show no such enrichment (*e.g.*, Kontak 1995), (2) the samples were run in several batches over a period of several months, (3) duplicate analyses gave similar results, and (4) standards run with the samples gave acceptable values. The role of a potential contaminant such as zircon also is ruled out, since insufficient Zr is present to satisfy mass-balance calculations assuming reasonable levels of REE in zircon grains, despite the positive correlation between Y and Zr (Fig. 4).

Two different chondrite-normalized REE patterns can

be distinguished for AF from pegmatites, on the basis of degree of fractionation. For AF in monzogranite-hosted pegmatite, there is LREE enrichment relative to chondrites, strong to moderate fractionation and, in general, a  $Eu_N/Eu^*$  value greater or equal to 1, whereas in AF from the more evolved pegmatites (types I, II), the pattern is less fractionated, the LREE enrichment is subtle, and  $Eu_N/Eu^*$  is close to 1. Also, note (1) some enrichment in the HREE in the monzogranite-hosted AF (*e.g.*, sample 40K), (2) a decrease in the abundance of the REE in AF from type-I to type-II pegmatites (except for sample 28.1), which is in keeping with the pattern of element enrichment noted above for these pegmatites (*e.g.*, Rb, Rb/Sr), and (3) the AF with the greatest enrichment in REE for type-I pegmatite is of metasomatic origin (sample 32; Kontak *et al.* 1996). The erratic profiles for some of the AF from type-II pegmatites (*e.g.*, 18.1) reflect levels of the rare earths close to their detection limits.

### A TEST OF ELEMENT MOBILITY

Most of the samples considered in this investigation were selected on the basis of lack of obvious hydrothermal effects. However, a single locality in the Halifax monzogranite was specifically selected to examine the importance of hydrothermal effects. The following alteration-related profile is observed (Fig. 7): (1) a central zone of silicified granite, where fine-grained quartz has replaced the monzogranite; (2) a zone in which all the biotite and the trace amounts of cordierite are replaced by chlorite, and (3) a zone where a hematite stain of the feldspar is prominent. Several such zones occur in the granite at this locality, and the alteration is similar to what is observed in many parts of the SMB that experienced focussed infiltration of an aqueous fluid phase. This pattern of alteration is commonly associated with uranium mineralization (*e.g.*, Logothetis 1985, Chatterjee *et al.* 1982).

In Figure 7, the composition of the alkali feldspar from a fresh sample of monzogranite (4A) is compared to an AF sample (4B) from the hematite-enriched halo; each sample was analyzed in duplicate. Regarding the trace elements other than the REE, reported as an average in Figure 7, there is little sign of mobility of Pb and Rb, a depletion of Li (55%), Sr, Ba and Cs (roughly 25% in each case), and a doubling of the Y content. The REE, with which yttrium commonly is grouped, also show an overall enrichment, increasing progressively with atomic number. However, the pattern is opposite for Eu, which presumably is depleted owing to the conversion of part of the structurally bound of  $Eu^{2+}$  to  $Eu^{3+}$ , in keeping with the appearance of hematite.

Another sample in this collection in which hydrothermal effects are suspected is 29B, taken from the Halifax monzogranite of the Halifax Pluton. It is from an area marginal to a muscovite – tourmaline – arsenopyrite greisen. The AF from this locality is noted

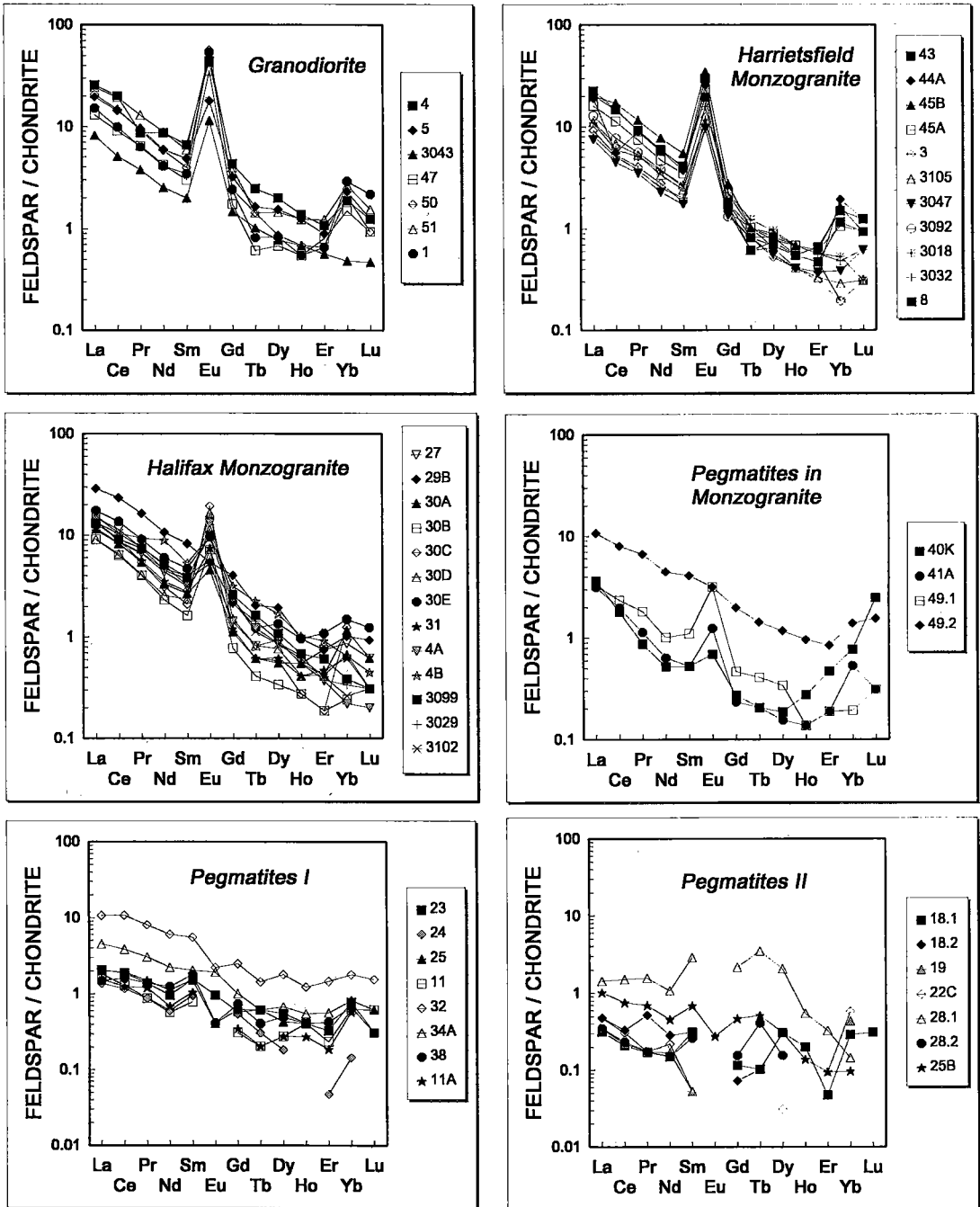


FIG. 6. Chondrite-normalized rare-earth-element plots for alkali feldspar separates from the eastern South Mountain Batholith. Note that for some alkali feldspar samples in type-II pegmatites, the scatter is related to the fact that some data approach analytical detection-limits for certain elements. Also note the change in scale for the pegmatite samples (types I and II).

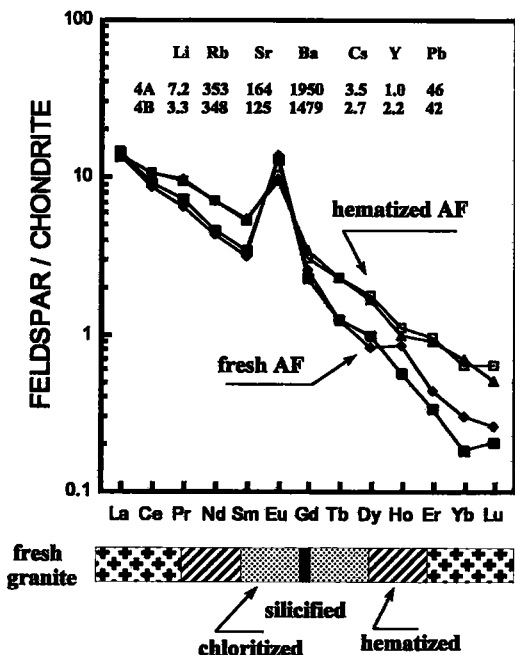


FIG. 7. Chondrite-normalized rare-earth-element plot for alkali feldspars from an alteration profile in the Halifax monzogranite. Sample 4A is from fresh granodiorite, whereas 4B is from the hematite-stained zone. The average trace-element contents for two samples of alkali feldspar from each zone are given in the plot.

for its relative depletion in Sr, Pb, elevated Rb/Sr ratio (Fig. 3k),  $\Sigma$ REE (Figs. 3n, 6) and LREE enrichment relative to other samples from the Halifax Pluton. Most of this variation may be related to elemental mobility related to the proximity of an alteration zone.

#### DISCUSSION

A consensus has emerged concerning broad petrogenetic questions in the evolution of the SMB, and the roles of fractional crystallization and of assimilation of crust-derived materials (Clarke & Muecke 1981, Clarke & Chatterjee 1988, Kontak *et al.* 1988, 1991, MacDonald & Clarke 1991, Clarke *et al.* 1993, Dostal & Chatterjee 1995, Tate & Clarke 1997). There are many questions that remain, in particular concerning the nature of the alkali feldspar, a major constituent of these rocks, and an important host of petrogenetically important trace-elements like Rb, Sr, and Pb. The alkali feldspar fraction of these rocks is more reactive than any other major rock-forming mineral. Whereas these rocks contain many minerals that crystallized directly from the relevant magmas, the alkali feldspar is not one of them. The material that we characterize here is merely a

pseudomorph of the primary feldspar (Martin 1988). During the pseudomorph-forming reactions, which involve  $H_2O$  as a necessary catalyst, challenging questions arise concerning the "openness" of the system and the degree to which the trace-element chemistry of the alkali feldspar has been modified. Not all the trace elements considered here are affected equally, and some clearly retain their magmatic distribution in the alkali feldspar. Thus the alkali feldspar fraction of the South Mountain Batholith can provide valuable insight into the relative importance of primary and secondary processes in defining the trace-element characteristics of this mineral and, by implication, of the whole-rock samples.

#### "Magmatic" part of the signature of alkali feldspar

Strontium and Ba are both incorporated in alkali feldspar by means of a coupled substitution, *e.g.*,  $Ba + Al \rightleftharpoons K + Si$ . Since the Al is tetrahedrally coordinated, it is impossible to mobilize Sr and Ba without tampering with the framework of the feldspar. As a result, we believe that the Sr and Ba recorded here represents the magmatic signature of the igneous rock. The plots of trace-element data indicate that in most cases, the AF in samples of granodiorite (so classified on the basis of proportions of normative constituents) contains the highest concentrations of Sr and Ba.

The first complication encountered is the incidence of overlap in the Sr and Ba concentrations in the alkali feldspar between granodiorite and monzogranite, with some separates of AF from the Harrietsfield monzogranite seemingly more primitive than those from granodioritic samples. It is well established that all calc-alkaline batholiths crystallize from many small batches of viscous magma. Such overlaps merely indicate that not all batches have the same proportions of feldspar-compatible elements prior to fractional crystallization. The geographic distribution of our samples (Fig. 1) ensures that we sampled products of crystallization from many batches of magma. Whereas all batches will follow the same general path of crystallization in the quinary system An–Ab–Or–Qtz– $H_2O$ , their starting points will differ in detail. Viewed in this light, the continuity of trends illustrated in Figures 3, 4, and 5 is really rather impressive.

In terms of Sr and Ba concentrations in the AF and its Rb/Sr value, the Harrietsfield monzogranite of the Halifax intrusive center consistently seems to be more primitive (*i.e.*, less fractionated) than the Halifax monzogranite. The two monzogranitic suites, which seem to grade one into the other where in contact (MacDonald & Horne 1988), may well have evolved from different parental magmas, or from the same parent but with a different proportion of crustal contaminant, the two coeval batches mixing along their interface. The important finding here is the AF of these two map-units offers a sensitive geochemical discriminant between the two types of monzogranite. Future studies could focus

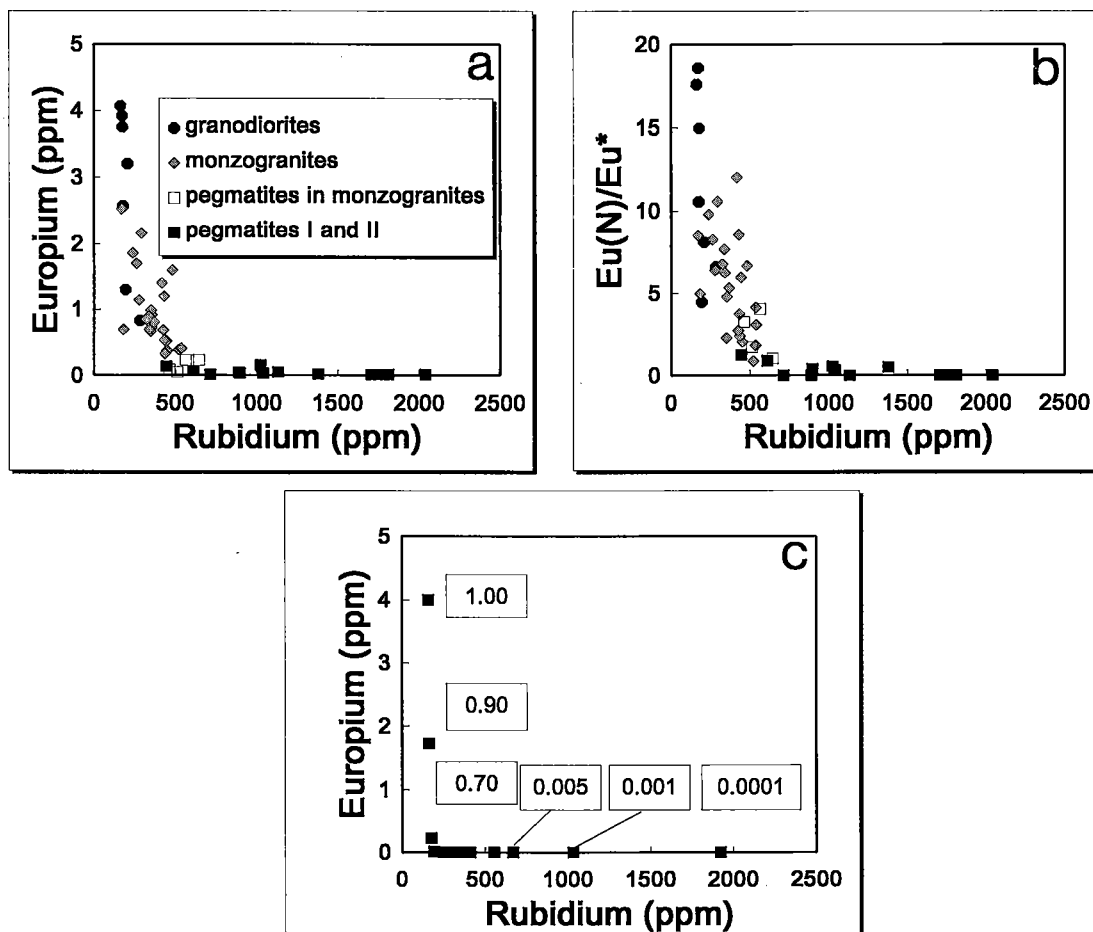


FIG. 8. Binary plot of Eu and  $Eu_N/Eu^*$  versus Rb for alkali feldspar separates, South Mountain batholith. The bottom plot is the trend calculated assuming Rayleigh crystal fractionation [equation in Hanson (1978)] and partition coefficients of Icenhower & London (1996) and Leeman & Phelps (1981) for Rb (0.63) and Eu (9), respectively. Numbers within the boxes are  $F$  values (*i.e.*, weight fraction of melt relative to the original parent); they indicate that only at very low melt fractions do the Rb contents measured approximate those calculated for the model (see text for discussion).

on the AF across the gradation between the Harrietsfield and Halifax monzogranites in order to address the petrogenetic questions raised.

An indirect test of the primary nature of the alkali feldspar's composition, at least in terms of Sr, Ba and Rb, can be made by checking whether the calculated "partition-coefficients" for these elements match published values for magmatic systems. The calculations are based on the average bulk-composition of AF in granodiorite and monzogranite hosts, and average whole-rock composition of samples in each grouping from the Halifax Pluton (MacDonald & Horne 1988). Results are 1.3 and 1 (Sr), 6 and 2 (Ba), and 1.2 and 2 (Rb), respectively. Although it is an important oversimplification to consider the whole rock to represent the magma that once coexisted with the alkali feldspar, these

findings are comparable to values given for other igneous systems (*e.g.*, McCarthy & Hasty 1976, Long 1978, Leeman & Phelps 1981, Walker *et al.* 1986, Stix & Gorton 1991). In the most recent experimental determination of these coefficients, Icenhower & London (1996) gave values of 10 to 14, 17.6 and 0.73 (Sr, Ba, and Rb, respectively, in the presence of  $Or_{70}$  in a peraluminous felsic magma). The partition coefficients for Ba and Rb were found to show a compositional dependence, which may explain why our inferred values for Ba and Rb show a greater range.

The plots of Sr, Ba and K/Rb versus Rb (Fig. 5) show evolutionary trends typical of those caused by Rayleigh crystal fractionation (*e.g.*, Arth 1976, Hanson 1978). The values of  $F$ , the proportion of melt remaining, calculated for each main group of samples, are in general accord

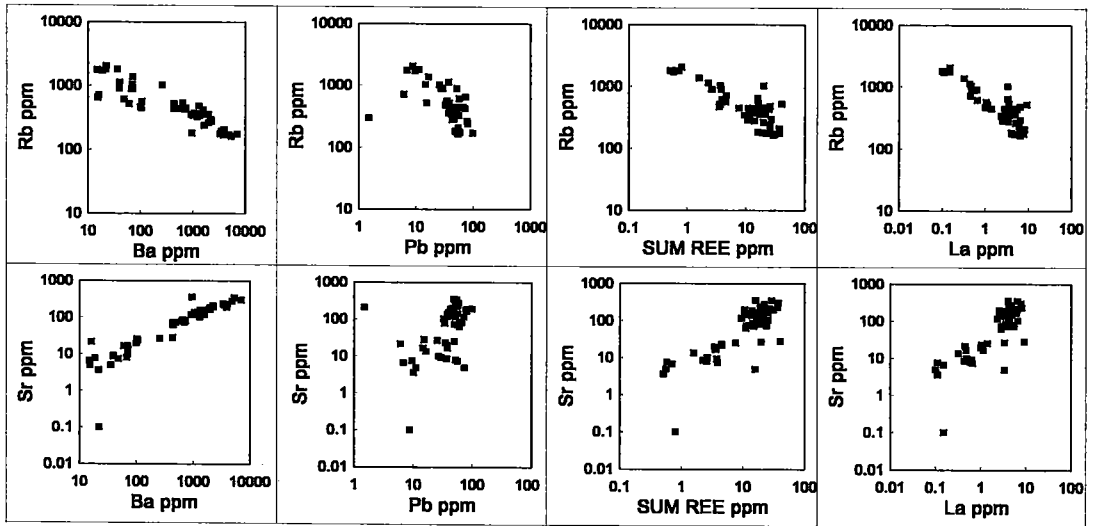


FIG. 9. Log-log plots for selected trace elements for alkali feldspar separates from the South Mountain batholith. The linear trends in such plots are interpreted to reflect the dominant role of Rayleigh crystal fractionation, as discussed for example by McCarthy & Hasty (1976) and Allègre *et al.* (1977) and in the text.

with the proportions of those rock types within the SMB. For example,  $F$  values are 0.1 to 0.2 for granodiorite, 0.5 for monzogranite and very low (to 0.0001) for the most evolved pegmatites. The values of  $F$  derived from the  $K/Ba$  versus  $Ba$  plot, calculated with the  $K_D$  value (17.6) of Icenhower & London (1996), contrast with the Rb- and Eu-based values (see below), most notably for AF from pegmatites. A much lower  $K_D(Ba)$  value ( $\leq 6$ ) would be required to satisfy the data (Fig. 5). Such a revised  $K_D$  value would conform more closely to empirical values derived for AF in natural assemblages (*e.g.*, Nash & Crecraft 1985, Smith & Brown 1988, Stix & Gordon 1991).

We contend that melt-crystal equilibria also controlled the observed distribution of the *REE* in these rocks; as in the case of Sr and Ba, the *REE* are incorporated in alkali feldspar *via* a coupled substitution, and thus are not easily dislodged during subsolidus fluid-circulation events. The chondrite-normalized concentrations of these elements in AF are virtually identical in all three of the more primitive units (Fig. 6), albeit with subtle differences in profile. Thus, fractional crystallization of the same assemblage of minerals probably controlled the distribution of the *REE* and, by extension, the abundance of such trace elements as Zr, Th and Y, in all three rock types. These elements are sequestered in accessory minerals that are strongly enriched in the *REE* (Gromet & Silver 1983, Bea 1996).

It is clear in Figure 6 that Eu, mostly present as  $Eu^{2+}$  in the magma, is much more compatible than all other

*REE* in the structure of the AF. In Figure 8, both the concentration of Eu and the magnitude of  $Eu_N/Eu^*$  are plotted as a function of Rb concentration. Both diagrams show the same trend, which is attributed to the initial rapid depletion of Eu. Such depletion can be modeled purely by feldspar fractionation, and reflects the systematic partition of  $Eu^{2+}$  into the AF (*e.g.*, Leeman & Phelps 1981, Smith & Brown 1988, Stix & Gorton 1991); note that the modeled  $F$  values shown in Figure 8 compare well with those calculated in Figure 5 on the basis of Sr and Ba [especially if a more moderate  $K_D(Ba)$  is selected]. Note that for the reason outlined above, there is considerable overlap of AF from granodiorite, monzogranite and monzogranite-hosted pegmatite. Also, the  $Eu_N/Eu^*$  values are markedly lower in AF from the Halifax monzogranite, which is chemically more evolved (Figs. 3, 4).

The geochemistry of the AF from the more evolved suites indicates a marked change from the granodiorite-monzogranite to the pegmatite stage, as noted previously in connection with Ba, Sr, Th, Rb/Sr, K/Rb, K/Ba and  $\Sigma REE$ . The AF from monzogranite-hosted pegmatites forms an intermediate population in terms of chemical composition (Figs. 3, 4, 5, 6) between AF in the samples of monzogranite and AF in leucogranite-hosted pegmatites. These findings suggest that the AF in these monzonite-hosted pegmatites also largely retains a magmatic signature.

In order to evaluate further the role of crystal-melt equilibria within the batholith, log-log plots (McCarthy

& Hasty 1976, Allègre *et al.* 1977, Cocherie 1986) are presented for selected elements in Figure 9. The linear trends involving the less mobile elements are well defined, and deviate most where levels of abundance approach the limits of detection. The trends are consistent with crystal (Rayleigh) fractionation, but do not exclude other processes (Nielsen 1990).

#### *Fluid-induced geochemical trends in the alkali feldspar*

The dispersion of data points in the Cs versus Rb plot (Fig. 4e) is inconsistent with fractional crystallization, and is considered indicative of AF–fluid interaction. As Lagache (1984) showed in her tabulation of partition coefficients  $D(\text{Cs})^{\text{AF/fluid}}$ , Cs is much more sensitive to low-temperature interaction than Rb. Thus equilibration of the magmatic feldspar as temperature decreases could be expected to lead to an increase in Rb/Cs. A similar trend occurs in the Pb–Rb plot (Fig. 4d); the points describing the AF in the less-evolved samples define a steep, essentially linear trend, whereas the AF in some pegmatitic samples show a large scatter, and enrichment in Pb or Rb (or both). A study of the Pb isotopes of the AF could be revealing in pinpointing the cause of the scatter in Figure 4d and in testing whether the mobility occurred at a magmatic temperature (melt–AF–fluid equilibrium) or is postmagmatic in origin. In their modeling of the alkali element evolution in the Tin Mountain (South Dakota) granitic pegmatites, Walker *et al.* (1986) made a case for magmatic crystallization in the presence of a fluid rather than under fluid-absent conditions, but there is no doubt that both Rb and Pb also can be mobilized at a lower temperature.

In Figure 8, the AF in some leucogranite-hosted pegmatites overlaps that in the most evolved monzogranite; a fluid phase seems to have been involved in both cases. The samples in the transition area are NS-85-27 (Halifax monzogranite) and NS-85-32 (hydrothermally deposited coarse AF, reported in Table 1 with group-I pegmatite). Sample NS-85-27, from a greisen zone, has retained its original bulk-composition (*ca.* Or<sub>65</sub>) and overall REE enrichment and chondritic patterns despite losing Eu, as evidenced by its present  $\text{Eu}_N/\text{Eu}^*$  value of 1; clearly the loss of Eu here was fluid-mediated, and probably can be attributed to oxidation of  $\text{Eu}^{2+}$ . Sample NS-85-32, which grew on a fracture surface, has a bulk composition Or<sub>92</sub> (Fig. 2); interestingly, it has a  $\Sigma\text{REE}$  and degree of fractionation comparable to those in the monzogranite host, but with a negative Eu anomaly. Here also, the  $\text{Eu}_N/\text{Eu}^*$  value might reflect the role of the fluid phase from which it deposited. There is no evidence in the SMB that low  $\text{Eu}_N/\text{Eu}^*$  values are in any way related to late-stage, fluid-induced albitization of the AF, as suggested by Fowler & Doig (1983) in their study of Eu anomalies in U- and Th-rich granites and pegmatites of Mont Laurier, Quebec.

Since the REE commonly forms the focus of alteration studies in mineralized felsic systems (*e.g.*, Taylor & Fryer 1980, 1983, White & Martin 1980), it is worth re-examining the behavior of the REE in terms of a fluid-mediated process. As alluded to before, the similar extent of depletion of the LREE and HREE has been modeled by fractionation of accessory phases (*e.g.*, Miller & Mittlefehldt 1982, Michael 1983, 1988), and a fluid phase need not be involved. Cases of fluid stripping of the REE in granite–pegmatite systems and alteration zones have been described (Breaks & Moore 1992, Taylor & Fryer 1983), and are supported by experimental evidence (*e.g.*, Flynn & Burnham 1978, D. London, pers. comm., 1997). By analogy with the aforementioned studies, the concave-upward chondrite-normalized REE profiles of the alkali feldspar in some pegmatitic samples (40K, 41A and 49.1; Fig. 6) may well be due to the action of a fluid phase.

The pegmatites emplaced in the leucogranites are a volumetrically very minor phase of the batholith, given that their progenitors, the leucogranites, may themselves only represent about 0.1 to 1% of the batholith by volume (MacDonald *et al.* 1992). In spite of this fact, there is in general no textural evidence that the relevant batches of evolved magma attained early saturation in an aqueous fluid phase. The Walker molybdenite locality provides the only exception; it shows crenulate layering of aplite, pegmatite, quartz-rich zones (comb quartz) and associated mineralization. In fact, Kirkham & Sinclair (1988) included this locality in their review of such phenomena, typically associated with actively degassing volatile-rich felsic magmas. London (1992) showed that the mere development of a pegmatitic texture should not be construed as a sign of saturation of a magma in an aqueous fluid. By the same token, it seems clear from the incidence of metasomatism and mineralization associated with the leucogranites, as well as from the increased incidence of microcline in the AF (see below), that there was indeed production of a fluid phase upon crystallization of the evolved magmas. The timing of the liberation of a gas phase is conjectural, but could perhaps be hinted at in a comparison of predicted and observed paths of fractionation.

The trace-element chemistry of the AF in the pegmatites may be used to infer that the fluid phase, and by extrapolation, the melt, was not enriched in F. In such a fluorine-enriched system, one could expect an enrichment in associated elements (*e.g.*, Zr, Th, HREE, *etc.*; Simmons *et al.* 1987, Campbell *et al.* 1995), and this would have been seen in the chemical signature of the AF (*e.g.*, Nassif & Martin 1992). Kontak (1995) documented HREE enrichment in AF of the fluorine-rich, high-silica Ackley Granite, in Newfoundland. This enrichment was attributed to the presence of a volatile phase prior to complete crystallization of the melt, with the HREE probably complexed in solution by fluoride complexes (Wood 1990).

*Subsolidus interaction of the magmatic alkali feldspar with a fluid phase*

The rocks that are described here no longer contain the magmatic alkali feldspar, but rather a pseudomorph that consists of orthoclase perthite in the granodiorite and monzogranite, and orthoclase  $\pm$  microcline perthite in the more evolved rocks (Kontak *et al.* 1996). Exsolution in the AF began as soon as the solid assemblage left the solidus. Only as the rock cooled below 450°C did the orthoclase host of the perthite begin to convert to microcline, by solution and redeposition in the presence of an aqueous pore fluid. Thus the successful conversion of orthoclase perthite to microcline perthite in the most evolved rocks is an indication that the entire potassium-rich feldspar was dissolved and reprecipitated, probably many times. Both exsolution and Al–Si ordering create pore space (Martin 1988), thus further facilitating the circulation of an aqueous fluid.

Details of the trace-element geochemistry are expected to be disturbed during this conversion if the fluid:rock ratio is great, for example in areas of mineralization and greisenization. Elsewhere, in instances of lower fluid:rock ratio, the scale of open-system behavior likely is strictly local. The localized destabilization of a primary accessory mineral that hosts the heavy rare-earths, *e.g.*, xenotime, in the presence of the aqueous fluid that catalyzes the exsolution and ordering reaction in the AF could well explain the unusual increase in the proportion of Yb and Lu in many of the AF fractions analyzed (Fig. 6). These are the most compatible of the rare earths; in spite of the lower temperatures and partition coefficients less than 1, it is reasonable to propose that the bulk of the Yb and Lu so liberated could be structurally bound in the two feldspars that make up the perthitic intergrowth. An extreme case of the same phenomenon may well be responsible for the progressive increase of the REE according to their atomic number in the wallrocks along paths of fluid circulation and active silicification (Fig. 7).

*Comparison to alkali feldspar chemistry of the Ackley Granite and the Harney Peak Granite*

Fields are indicated in Figure 4 for the AF from the high-silica, highly evolved Ackley Granite, Newfoundland (Tuach *et al.* 1986, Kontak 1995). Note that those data were acquired according to the same protocol and with the same analytical equipment as the data reported in this investigation. No data are available for AF from pegmatites in the Ackley suite. In spite of this shortcoming, it is clear that: 1) the Ackley data define a different trajectory in a Sr–Rb plot, indicative of a significantly greater enrichment in Rb in the Ackley suite, even in its relatively mafic members. 2) In plots of Pb–Rb and Ba–Rb, the two suites generally overlap; the SMB contains more primitive rocks, to judge from the Ba content of its alkali feldspar. 3) Both suites display

approximately the same abundances of trace elements in the AF of non-pegmatitic samples, although the Ackley AF show slightly higher amounts of Rb, in keeping with whole-rock data, indicating that the batches of magma at Ackley were more rare-alkali-enriched. This is also apparent in the range of Rb/Sr values, 15 to 20 in AF from the Ackley suite compared to 5 to 10 in AF from non-pegmatitic samples of the SMB. 4) There is good agreement between the two data sets in the Cs–Rb plot (not shown); these elements were similarly partitioned into AF in the two suites, despite the fact that the bulk compositions were dissimilar (*e.g.*, the SMB is strongly peraluminous compared to the Ackley). 5) Kontak (1995) showed that the AF from the Ackley granite is enriched in Zr (10 to 30 ppm), Th (3 to 12 ppm) and Mo (10 to 40 ppm) compared to AF from the SMB suite.

In the Ba–Rb plot (Fig. 4b), the trend for AF from the Harney Peak Granite is shown to be displaced from both the SMB and the Ackley Granite, which indicates a different bulk-composition of the melt, distinctly more enriched in Rb for a given Ba content. The alkali feldspar is a sensitive geochemical indicator of either source characteristics or magmatic processes in these three granitic suites.

#### CONCLUSIONS

The geochemistry of alkali feldspar separates from the granodiorite – monzogranite – pegmatite phases of the eastern part of the South Mountain Batholith (SMB), southern Nova Scotia, indicates a continuous, systematic change in the trace elements that follows patterns previously defined by whole-rock chemistry. For example, the levels of Ba, Sr, Pb, Zr, Th and  $\Sigma REE$ , and the magnitude of K/Rb, decrease from granodiorite to granitic pegmatite, whereas Rb, Cs and K/Ba increase. Trends in binary plots and in terms of ratios of concentrations mimic those predicted for Rayleigh crystal fractionation. The same inference is made from linear trends in log–log plots. Models of the trace-element data, assuming Rayleigh fractional crystallization, indicate *F* values generally consistent with the proportion of rock types within the SMB. *F* values based on K/Ba variation are somewhat aberrant, and may reflect an inappropriate choice of  $K_D(Ba)$  value. Although the decrease in  $\Sigma REE$  and the systematic change in chondrite-normalized REE patterns are consistent with fractionation of accessory mineral phases, as demonstrated in model calculations, the common enrichment in Yb and Lu in AF from all rock types, and the shape of the chondrite-normalized REE pattern in a few samples of AF from pegmatitic samples, suggest that some fluid-mediated mobilization has occurred. Other elements less tightly held in the feldspar structure, in particular Cs, Rb and part of the Pb, are subject to open-system behavior, though not necessarily on a large scale. The conversion of the magmatic alkali feldspar to orthoclase perthite and, in the case of the more evolved rocks, to microcline perthite, involves dissolution

steps in an aqueous fluid medium. It is likely that the trace-element signature is easily reset at this stage. Comparison of the AF data for the SMB with AF from the high-silica Ackley Granite, Newfoundland, and the Harney Peak Granite, South Dakota, indicate that the AF is a sensitive geochemical marker of different source-regions or different petrogenetic processes at the magmatic stage, as long as the hydrothermal modifications are taken into account.

#### ACKNOWLEDGEMENTS

This study was begun while the first author was in residence at the Memorial University of Newfoundland, and was financed by an NSERC operating grant to Dr. D.F. Strong. Data were acquired with the capable assistance of Drs. S.J. Jackson and H. Longrich of Memorial University. Reviews of the paper by J. Dostal and two referees resulted in substantial improvements. Samples were collected with the assistance of the SMB gang; their exchange of ideas concerning the evolution of the SMB over the past decade is greatly appreciated.

#### REFERENCES

- ALLÈGRE, C.J., TREUIL, M., MINSTER, J.-F., MINSTER, B. & ALBARÈDE, F. (1977): Systematic use of trace element in igneous process. I. Fractional crystallization processes in volcanic suites. *Contrib. Mineral. Petrol.* **60**, 57-75.
- ARTH, J.G. (1976): Behavior of trace elements during magmatic processes – a summary of theoretical models and their application. *J. Res. U.S. Geol. Surv.* **4**, 41-47.
- BEA, F. (1996): Residence of REE, Y, Th and U in granites and crustal protoliths; implications for the chemistry of crustal melts. *J. Petrol.* **37**, 521-552.
- BREAKS, E.F. & MOORE, J.M., JR. (1992): The Ghost Lake Batholith, Superior Province of northwestern Ontario: a fertile, S-type, peraluminous granite – rare-element pegmatite system. *Can. Mineral.* **30**, 835-876.
- CAMPBELL, A.R., BANKS, D.A., PHILLIPS, R.S. & YARDLEY, B.W.D. (1995): Geochemistry of the Th–U–REE mineralizing magmatic fluids, Capitan Mountains, New Mexico. *Econ. Geol.* **90**, 1271-1287.
- CARRON, J.-P. & LAGACHE, M. (1980): Etude expérimentale du fractionnement des éléments Rb, Cs, Sr et Ba entre feldspaths alcalins, solutions hydrothermales et liquides silicatés dans le système Q.Ab.Or.H<sub>2</sub>O à 2 kbar entre 700 et 800°C. *Bull. Minéral.* **103**, 571-578.
- ČERNÝ, P. (1992): Geochemical and petrogenetic features of mineralization in rare-element granitic pegmatites in the light of current research. *Appl. Geochem.* **7**, 393-416.
- \_\_\_\_\_ (1994): Evolution of feldspars in granitic pegmatites. In *Feldspars and Their Reactions* (I. Parsons, ed.). Kluwer Academic Publ., Rotterdam, The Netherlands (501-540).
- \_\_\_\_\_, MEINTZER, R.F. & ANDERSON, A.J. (1985): Extreme fractionation in rare-element granitic pegmatites: selected examples of data and mechanisms. *Can. Mineral.* **23**, 381-421.
- \_\_\_\_\_, SMITH, J.V., MASON, R.A. & DELANEY, J.S. (1984): Geochemistry and petrology of feldspar crystallization in the Vezná pegmatite. *Can. Mineral.* **22**, 381-421.
- CHATTERJEE, A.K., ROBERTSON, J. & POLLOCK, D. (1982): A summary of the petrometallogenesis of the uranium mineralization at Millet Brook, South Mountain Batholith. *Nova Scotia Dep. Mines & Energy, Rep.* **82-1**, 57-66.
- CLARKE, D.B. & CHATTERJEE, A.K. (1988): Physical and chemical processes in the South Mountain Batholith. In *Recent Advances in the Geology of Granite-Related Mineral Deposits* (R.P. Taylor & D.F. Strong, eds.). *Can. Inst. Mining Metall., Spec. Vol.* **39**, 223-233.
- \_\_\_\_\_, MCKENZIE, C.B., MUECKE, G.K. & RICHARDSON, S.W. (1976): Magmatic andalusite from the South Mountain Batholith, Nova Scotia. *Contrib. Mineral. Petrol.* **56**, 279-287.
- \_\_\_\_\_, & MUECKE, G.K. (1981): Geochemical evolution of the South Mountain Batholith, Nova Scotia: rare earth elements. *Can. Mineral.* **19**, 133-146.
- \_\_\_\_\_, & \_\_\_\_\_ (1985): Review of the petrochemistry and origin of the South Mountain Batholith and associated plutons, Nova Scotia, Canada. In *High Heat Production (HHP) Granites: Hydrothermal Circulation and Ore Genesis*. Inst. Mining and Metallurgy, London, U.K. (41-54).
- \_\_\_\_\_, REYNOLDS, P.H., MACDONALD, M.A. & LONGSTAFFE, F. (1993): Leucogranites from the eastern part of the South Mountain Batholith, Nova Scotia. *J. Petrol.* **34**, 653-679.
- COCHERIE, A. (1986): Systematic use of trace element distribution patterns in log-log diagrams for plutonic suites. *Geochim. Cosmochim. Acta* **50**, 2517-2522.
- DOSTAL, J. & CHATTERJEE, A.K. (1995): Origin of topaz-bearing and related peraluminous granites of the Late Devonian Davis Lake pluton, Nova Scotia: Canada: crystal versus fluid fractionation. *Chem. Geol.* **123**, 67-88.
- FLYNN, R.T. & BURNHAM, C.W. (1978): An experimental determination of rare earth partition coefficients between a chloride containing vapor phase and silicate melts. *Geochim. Cosmochim. Acta* **42**, 685-701.
- FOWLER, A.D. & DOIG, R. (1983): The significance of europium anomalies in the REE spectra of granites and pegmatites, Mont Laurier, Quebec. *Geochim. Cosmochim. Acta* **47**, 1131-1137.
- GOAD, B.E. & ČERNÝ, P. (1981): Peraluminous pegmatitic granites and their pegmatite aureoles in the Winnipeg River district, southeastern Manitoba. *Can. Mineral.* **19**, 177-194.
- GROMET, L.P. & SILVER, L.T. (1983): Rare earth element distributions among minerals in a granodiorite and their

- petrogenetic implications. *Geochim. Cosmochim. Acta* **47**, 925-939.
- HANSON, G.N. (1978): The application of trace elements to the petrogenesis of igneous rocks of granitic composition. *Earth Planet. Sci. Lett.* **38**, 26-43.
- ICENHOWER, J. & LONDON, D. (1996): Experimental partitioning of Rb, Cs, Sr, and Ba between alkali feldspar and peraluminous melt. *Am. Mineral.* **81**, 719-734.
- JAHNS, R.H. & BURNHAM, C.W. (1969): Experimental studies of pegmatite genesis. I. A model for the derivation and crystallization of granitic pegmatites. *Econ. Geol.* **64**, 843-864.
- JENNER, G.A., LONGERICH, H.P., JACKSON, S.E. & FRYER, B.J. (1990): ICP-MS – a powerful tool for high precision trace element analyses in earth sciences: evidence from analysis of selected USGS reference samples. *Chem. Geol.* **83**, 133-148.
- KIRKHAM, R.V. & SINCLAIR, W.D. (1988): Comb quartz layers in felsic intrusions and their relationship to porphyry deposits. In *Recent Advances in the Geology of Granite-Related Mineral Deposits* (R.P. Taylor & D.F. Strong, eds.). *Can. Inst. Mining Metall., Spec. Vol.* **39**, 50-71.
- KONTAK, D.J. (1995): A study of feldspar phases in the high-silica, high-level Ackley Granite, southeastern Newfoundland. *Can. Mineral.* **33**, 985-1010.
- \_\_\_\_\_, & COREY, M.C. (1988): Metasomatic origin for spessartine-rich garnet in the South Mountain Batholith, Nova Scotia. *Can. Mineral.* **26**, 315-334.
- \_\_\_\_\_, KERRICH, R. & STRONG, D.F. (1991): The role of fluids in the late-stage evolution of the South Mountain Batholith, Nova Scotia: further geochemical and oxygen isotopic studies. *Atlantic Geol.* **27**, 29-47.
- \_\_\_\_\_, MARTIN, R.F. & RICHARD, L. (1996): Patterns of phosphorus enrichment in alkali feldspar, South Mountain Batholith, Nova Scotia, Canada. *Eur. J. Mineral.* **8**, 805-824.
- \_\_\_\_\_, & STRONG, D.F. (1988): Geochemical studies of alkali feldspar in lithophile element-rich granite suites from Newfoundland, Nova Scotia and Peru. *Geol. Assoc. Can. – Mineral. Assoc. Can., Program Abstr.* **13**, A68.
- \_\_\_\_\_, \_\_\_\_\_ & KERRICH, R. (1988): Crystal-melt + fluid phase equilibria versus late-stage fluid:rock interaction in granitoid rocks of the South Mountain Batholith, Nova Scotia: whole rock geochemistry and oxygen isotope evidence. *Mar. Sed. & Atlantic Geol.* **24**, 97-110.
- LAGACHE, M. (1984): The exchange equilibrium distribution of alkali and alkaline-earth elements between feldspars and hydrothermal solutions. In *Feldspars and Feldspathoids* (W.L. Brown, ed.). D. Reidel Publ. Co., Boston, Massachusetts (247-280).
- \_\_\_\_\_, & QUÉMÉNEUR, J. (1997): The Volta Grande pegmatites, Minas Gerais, Brazil: an example of rare-element pegmatites exceptionally enriched in lithium and rubidium. *Can. Mineral.* **35**, 153-165.
- LEEMAN, W.P. & PHELPS, D.W. (1981): Partitioning of rare earth and other trace elements between sanidine and coexisting volcanic glass. *J. Geophys. Res.* **86**, 10193-10199.
- LOGOTHETIS, J. (1985): Economic geology of the New Ross – Vaughan complex. In *Guide to the Granites and Mineral Deposits of Southwestern Nova Scotia* (A.K. Chatterjee & D.B. Clarke, eds.). *Nova Scotia Dep. Mines & Energy, Pap.* **85-3**, 41-62.
- LONDON, D. (1992): The application of experimental petrology to the genesis and crystallization of granitic pegmatites. *Can. Mineral.* **30**, 499-540.
- LONG, P.E. (1978): Experimental determination of partition coefficients for Rb, Sr, and between alkali feldspar and silicate liquid. *Geochim. Cosmochim. Acta* **42**, 833-846.
- MACDONALD, M.A. & CLARKE, D.B. (1991): Use of nonparametric ranking statistics to characterize magmatic and post-magmatic processes in the eastern South Mountain batholith, Nova Scotia. *Chem. Geol.* **92**, 1-20.
- \_\_\_\_\_, COREY, M.C., HAM, L.J. & HORNE, R.J. (1992): An overview of recent bedrock mapping and follow-up petrological studies of the South Mountain Batholith, southwestern Nova Scotia. *Atlantic Geol.* **28**, 7-28.
- \_\_\_\_\_, & HORNE, R.J. (1988): Petrology of the zoned, peraluminous Halifax Pluton, south-central Nova Scotia. *Mar. Sed. & Atlantic Geol.* **24**, 33-46.
- MARTIN, R.F. (1988): The K-feldspar mineralogy of granites and rhyolites: a generalized case of pseudomorphism of the magmatic phase. *Rend. Soc. Ital. Mineral. Petrol.* **43**, 343-354.
- MCCARTHY, T.S. & HASTY, R.A. (1976): Trace element distribution patterns and their relationship to the crystallization of granitic melts. *Geochim. Cosmochim. Acta* **40**, 1351-1358.
- MICHAEL, P.J. (1983): Chemical differentiation of the Bishop Tuff and other high-silica magmas through crystallization processes. *Geology* **11**, 31-34.
- \_\_\_\_\_, (1988): Partition coefficients for rare earth elements in mafic minerals of high silica rhyolites: the importance of accessory mineral inclusions. *Geochim. Cosmochim. Acta* **52**, 275-282.
- MILLER, C.F. & MITTFELDELT, D.W. (1982): Depletion of light rare-earth elements in felsic magmas. *Geology* **10**, 129-133.
- NASH, W.P. & CRECRAFT, H.R. (1985): Partition coefficients for trace elements in silicic magmas. *Geochim. Cosmochim. Acta* **49**, 2309-2322.
- NASSIF, G.J. & MARTIN, R.F. (1992): Feldspar mineralogy of the Strange Lake peralkaline complex, Quebec-Labrador. *Geol. Assoc. Can. – Mineral. Assoc. Can., Program Abstr.* **17**, A83.
- NIELSEN, R.L. (1990): Simulation of igneous differentiation processes. In *Modern Methods of Igneous Petrology: Understanding Magmatic Processes* (J. Nicholls & J.K. Russell, eds.). *Rev. Mineral.* **24**, 65-105.

- RAESIDE, R.P. & MAHONEY, K.M. (1996): The contact metamorphic aureole of the South Mountain Batholith, southern Nova Scotia. *Geol. Assoc. Can. – Mineral. Assoc. Can., Program Abstr.* **21**, A77.
- REYNOLDS, P.H., ELIAS, P., MUECKE, G.K. & GRIST, A.M. (1987): Thermal history of the southwestern Meguma Zone, Nova Scotia from an  $^{40}\text{Ar}/^{39}\text{Ar}$  and fission track dating study of intrusive rocks. *Can. J. Earth Sci.* **24**, 1952-1965.
- SHEARER, C.K., PAPIKE, J.J. & JOLLIFF, B.L. (1992): Petrogenetic links among granites and pegmatites in the Harney Peak rare-element granite-pegmatite system, Black Hills, South Dakota. *Can. Mineral.* **30**, 785-809.
- \_\_\_\_\_, \_\_\_\_\_ & LAUL, J.C. (1987): Mineralogical and chemical evolution of a rare-element granite-pegmatite system: Harney Peak granite, Black Hills, South Dakota. *Geochim. Cosmochim. Acta* **51**, 473-486.
- SIMMONS, W.B., LEE, M.T. & BREWSTER, R.H. (1987): Geochemistry and evolution of the South Platte granite-pegmatite system, Jefferson County, Colorado. *Geochim. Cosmochim. Acta* **51**, 455-471.
- SMITH, J.V. (1974): *Feldspar Minerals. 2. Chemical and Textural Properties*. Springer-Verlag, Heidelberg, Germany.
- \_\_\_\_\_. (1983): Some chemical properties of feldspars. In *Feldspar Mineralogy* (second edition, P.H. Ribbe, ed.). *Rev. Mineral.* **2**, 281-296.
- \_\_\_\_\_. & BROWN, W.L. (1988): *Feldspar Minerals. 1. Crystal Structures, Physical, Chemical, and Microtextural Properties*. Springer Verlag, New York, N.Y.
- STEVENSON, R.K. & MARTIN, R.F. (1986): Implications of the presence of amazonite in the Broken Hill and Geco metamorphosed sulfide deposits. *Can. Mineral.* **24**, 729-745.
- STIX, J. & GORTON, M.P. (1991): Variations in trace element partition coefficients in sanidine in the Cerro Toledo Rhyolite, Jemez Mountains, New Mexico: effects of composition, temperature, and volatiles. *Geochim. Cosmochim. Acta* **54**, 2697-2708.
- TATE, M.C. & CLARKE, D.B. (1997): Compositional diversity among Late Devonian peraluminous granitoid intrusions in the Meguma Zone of Nova Scotia, Canada. *Lithos* **39**, 179-194.
- TAYLOR, R.P. & FRYER, B.J. (1980): Multiple-stage hydrothermal alteration in porphyry copper systems in northern Turkey: the temporal interplay of potassic, propylitic and phyllic fluids. *Can. J. Earth Sci.* **17**, 901-926.
- \_\_\_\_\_. & \_\_\_\_\_ (1983): Rare earth element litho geochemistry of granitoid mineral deposits. *Can. Inst. Mining. Metall., Bull.* **76**(860), 74-84.
- TUACH, J., DAVENPORT, P.H., DICKSON, W.L. & STRONG, D.F. (1986): Geochemical trends in the Ackley Granite, southeast Newfoundland: their relevance to magmatic – metallogenic processes in high-silica granitoid systems. *Can. J. Earth Sci.* **23**, 747-765.
- WALKER, R.J., HANSON, G.N., PAPIKE, J.J., O'NEIL, J.R. & LAUL, J.C. (1986): Internal evolution of the Tin Mountain pegmatite, Black Hills, South Dakota. *Am. Mineral.* **71**, 440-459.
- WHITE, M.V.W. & MARTIN, R.F. (1980): The metasomatic changes that accompany uranium mineralization in the nonorogenic rhyolites of the Upper Aillik Group, Labrador. *Can. Mineral.* **18**, 459-479.
- WOOD, S.A. (1990): The aqueous geochemistry of the rare-earth elements and yttrium. 2. Theoretical predictions of speciation in hydrothermal solutions to 350°C at saturation water vapor pressure. *Chem. Geol.* **88**, 99-115.

Received July 14, 1996, revised manuscript accepted May 30, 1997.